Tribology Letters (2023) 71:41
https://doi.org/10.1007/s11249-023-01714-7

ORIGINAL PAPER

Linking Molecular Structure and Lubrication Mechanisms in Tetraalkylammonium Orthoborate Ionic Liquids

Jieming Yan[1,2] · Hsu-Ming Lien[1,2] · Filippo Mangolini[1,3]

Received: 18 February 2023 / Accepted: 20 February 2023

Abstract

While ionic liquids (ILs) have gained wide interest as potential alternative lubricants able to meet the requirements of next-generation tribological systems owing to their unique physico-chemical properties and promising lubricating behavior, our understanding of the mechanisms by which ILs reduce friction and/or wear is still elusive. Here, we combine macroscale tribological experiments with surface-analytical measurements to shed light on the lubrication mechanisms of a class of halogen-free ILs, namely tetraalkylammonium orthoborate ILs, at steel/steel sliding contacts. The tribological results indicate an improvement of the friction-reducing properties of these ILs as the length of the alkyl chains attached to ammonium cations increases. X-ray photoelectron spectroscopy analyses provide further evidence for the dependence of the lubrication mechanism of tetraalkylammonium orthoborate ILs on the IL structure. In the case of tetraalkylammonium orthoborate ILs with asymmetric ammonium cations containing a long alkyl chain, no sacrificial tribofilms were formed on steel surfaces, thus suggesting that the friction-reducing ability of these ILs originates from their propensity to undergo a pressure-induced morphological change at the sliding interface that leads to the generation of a lubricious, solid-like layered structure. Conversely, the higher friction response observed in tribological tests performed with tetraalkylammonium orthoborate ILs containing more symmetric ammonium cations and short alkyl chains is proposed to be due to the inability of this IL to create a transient interfacial layer owing to the reduced van der Waals interactions between the cationic alkyl chains. The resulting hard/hard contact between the sliding surfaces is proposed to lead to the cleavage of boron-oxygen bonds in the presence of water to form species that then adsorb onto the steel surface, including trivalent borate esters and oxalic acid from the decomposition of orthoborate anions, as well as tertiary amines from the degradation of alkylammonium cations induced by hydroxides released during the orthoborate decomposition reaction. The results of this work not only establish links between the molecular structure of a class of halogen-free ILs, their lubricating performance, and lubrication mechanism, but also provide evidence for the existence of multiple mechanisms underpinning the promising lubricating properties of ILs in general.

Graphical Abstract

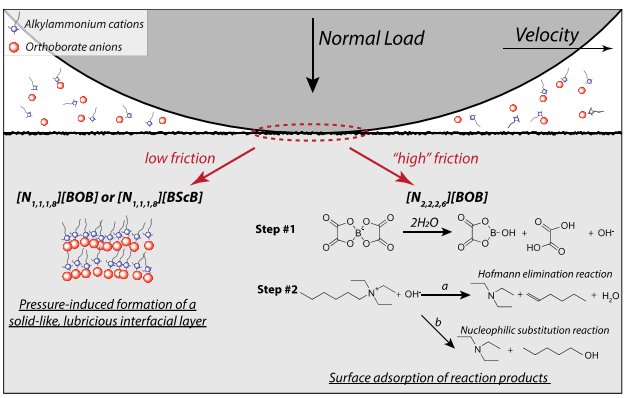

Extended author information available on the last page of the article

Published online: 04 March 2023

Keywords Ionic liquids · Borates · Lubricant additives · Boundary lubrication · Tribochemistry · X-ray photoelectron spectroscopy

1 Introduction

Among the several additives commonly employed to blend engine oils with, surface-active molecules able to adsorb on material surfaces and create low-shear-strength interfaces are normally used with the aim of reducing friction and/or wear [1]. Even though phosphorus- and sulphur-based friction-modifiers and anti-wear additives have been employed with success for decades, their decomposition under engine operating conditions results in chemical species containing high levels of metallic ashes along with phosphorus and sulphur oxides, which degrade the efficiency of exhaust after-treatment catalysts and filters [2]. Consequently, engine-lubricant specifications have progressively decreased the permissible content of sulphated ash, phosphorus, and sulphur (SAPS) in oils [2, 3]. While the concentration of additives containing all three catalyst-poisoning agents, such as zinc dialkyldithiophosphates (ZDDPs), has been reduced over the years [4], significant efforts have been spent in the development of novel additives with lower- or zero-SAPS level [2]. In addition to several published studies focusing on the evaluation of ashless equivalents to ZDDPs, such as thiophosphates or phosphates without any metals, as potential replacement or supplement to ZDDPs [5–8], a number of zero-SAPS additives has also been investigated, including nitrogen- and oxygen-heterocyclic compounds, halides, and nanoparticles [2]. Among them, boron-containing compounds have attracted considerable attention in tribology, as highlighted by a recent review on the topic [9]. Even though organoboron compounds were known to be effective corrosion inhibitors, it was not until the 1960s that their anti-wear properties were recognized [2]. Notably, Kreuz et al. highlighted, for the first time, that the extreme-pressure performance of tribenzylborate derives from its ability of forming a 100–200 nm thick, hard film containing boric and ferrous oxides [10]. Subsequent investigations by Liu et al. provided evidence for the good friction-reducing and anti-wear performance of a series of triborate esters [11, 12]. Even though X-ray photoelectron spectroscopy (XPS) analyses did not indicate the formation of boron oxide (B_2O_3) or boron hydroxide $B(OH)_3$, the spectroscopic results suggested the loss of alkyl groups attached to boron. More recently, Philippon et al. evaluated the tribochemical reaction of trimethylborate (TMB) at steel/steel interfaces under gas-phase conditions [13] and interpreted the experimental results on the basis of Pearson's hard and soft acid and base (HSAB) principle [14–17]: the scission of carbon–oxygen (C–O) bonds in TMB induced by the friction process was proposed to lead to the formation of a "borderline" base (*i.e.*, BO_3^{3-}), which can react with "borderline" acids (*i.e.*, Fe^{3+} and Fe^{2+}) to form a reaction layer made of a borate glass network with digested abrasive iron oxide that reduces friction and wear. Despite these promising results, trivalent borate esters are electron deficient and have a vacant p-orbital, which makes them electrophilic and susceptible to hydrolysis [2, 9]. While significant efforts have been spent in improving the resistance of organic borates to hydrolysis by improving their chemical architecture to inhibit the attack of water molecules [2, 18–23], the hydrolytic instability of trivalent organoborates has hindered their wider used in tribological applications.

In the last two decades, technological developments in the transportation sector, which resulted in vehicle electrification, together with growing demands for enhancing sustainable development have brought about a need for "green" lubricants with improved functionalities. As highlighted by several reviews [24–28], ionic liquids (ILs), which are ionic compounds with melting temperature below 373 K [29], have gained wide interest as potential alternative lubricants able to meet the requirements of next-generation tribological systems. The attractive physico-chemical properties of ILs, such as high thermal stability, low flammability, low vapor pressure, and high degree of chemical tunability [30–33], combines with their strong interaction with material surfaces owing to their ionic nature, which has opened novel paths for tailoring their lubricity by controlling the structure of the IL boundary layers [34–40].

Several studies highlighted the good lubricating properties of neat ILs [41–47], which, in some cases, even outperform the one of commercially used fully-formulated oils [43, 44, 48]. Despite these promising results, the implementation of ILs in oil formulations has been constrained by four main issues: (i) their high cost; (ii) the corrosivity of most ILs, which derives from the sensitivity of halogenated ILs to moisture that can result in the release of toxic and corrosive halogen halides [49–52]; (iii) the limited solubility of the vast majority of ILs in hydrocarbon fluids; and (iv) our limited understanding of the IL lubrication mechanism(s), which has hampered our ability of rationally designing task-specific ILs [53]. The first three issues have progressively been solved over the last decade with: (i) the recent synthesis of air-stable, eco-friendly, protic ILs (PILs), whose ease of preparation can significantly lower costs [54, 55]; (ii) the transition towards halogen-free ILs, which has drastically decreased corrosion problems [56–65]; and (iii) the

synthesis of oil-soluble ILs [31, 61, 66–72] and the development of polymer-encapsulated ILs [53]. Despite these remarkable advancements, the underpinning lubrication mechanism of ILs is still under debate. Surface force apparatus (SFA) and colloidal atomic force microscopy (cAFM) studies demonstrated that, in the absence of mechanochemical reactions (at low normal pressures, *i.e.*, < 100 MPa), ILs form layered ionic structures when nanoconfined between model, smooth surfaces [27, 28, 73–76], while also highlighting a strong dependence of the properties of the interfacial layers on the molecular architecture of the ILs, the water content in ILs, the chemistry of the solid surfaces, and the applied electrical potential [26, 27]. To evaluate the response of phosphorus-based ILs at higher contact pressure (> 500 GPa), Li et al. recently performed in situ AFM experiments and provided evidence that the lubrication mechanism of phosphonium phosphate ILs (PP-ILs) strongly depends on the applied normal pressure [77, 78]. At an applied pressure below 5.5 ± 0.3 GPa, a lubricious, quasi-solid interfacial layer forms as a result of the pressure-induced morphological change of confined ILs [77], while at normal pressures between 5.5 ± 0.3 GPa and 7.3 ± 0.4 GPa the progressive removal of the oxide layer from the steel surface leads to the adsorption of phosphate ions on metallic iron surface, which was proposed to generate a densely-packed, boundary layer that reduces nanoscale friction [78]. Macroscale tribological experiments in the boundary-lubrication regime, however, provided evidence that ILs can tribochemically react on metallic surfaces [24, 31, 32, 44, 66, 67, 79–85]. As a particular example, phosphorus-based ILs could form phosphate tribofilms on iron surfaces [31, 66, 67] in a similar manner to other anti-wear organo-phosphates [86, 87]. Li et al. recently reconciled the apparent disagreement between published macroscale and nanoscale tribological studies carried out with PP-ILs: the significantly different contact conditions in nanoscale and macroscale tests result in completely different temperature profiles at the contact (*i.e.*, a significant rise in contact temperature (up to 413 K) occurred in macroscale experiments due to the high sliding speeds, while a negligible interfacial temperature change occurs in nanoscale tests due to the low sliding speeds), which enhance the kinetics of tribochemical reactions only at macroscale contacts [78].

In the last few years, a novel class of halogen-free ILs including phosphonium cations and orthoborate anions has extensively been employed for fundamental studies in lubrication science [47, 58, 65, 88, 89]. Notably, Rohlmann et al. evaluated the lubricating performance of trihexyl(tetradecyl) phosphonium bisoxalatoorthoborate (P-BOB) at 353 K and 413 K in steel/steel contacts and proposed, on the basis of infrared spectroscopy measurements, that the decomposition of bisoxalatoorthoborate anions occurs through the scission of boron-oxygen bonds and results in the formation of oxalates that can easily adsorb on iron surfaces and reduce friction [88]. Additionally, the authors detected by energy-dispersive X-ray spectroscopy the presence of an increased oxygen and boron content together with phosphorus inside the wear tracks, which was interpreted as an indication for the potential formation of iron(III) borate mixed with iron oxalate as well as boron phosphate. Despite the relevance of this study, a full mechanistic description of the lubrication mechanism(s) of boron-containing ILs is still lacking and calls for the exploitation of surface-analytical techniques, such as XPS, to quantitatively determine the elements' bonding configuration in the near-surface region with the aim of shedding light on the elementary processes occurring at sliding interfaces. It has to be highlighted that, even though phosphonium orthoborate ILs have extensively been studied, the chemistry of this class of ILs poses significant challenges for fundamental tribochemical studies owing to the presence of two glass-forming elements, namely phosphorous and boron, that have overlapping XPS signals (B 1 s and P 2 s).

To address this challenge and gain new insights into the mechanism by which halogen-free orthoborate ILs reduce friction and/or wear in steel/steel contacts, we herein synthesize tetraalkylammonium orthoborate ILs. The results of macroscale tribological testing, combined with XPS measurements, indicated that the structure of the tetraalkylammonium cations affects the IL ability of forming a mechanically stable, transient boundary layer. In particular, tetraalkylammonium orthoborate ILs with symmetric cations having short alkyl chains are not effective in reducing friction and preventing the decomposition of orthoborate anions, which results in the surface adsorption of borate esters and oxalic acid together with amines formed by the degradation of quaternary ammonium ions.

2 Materials and Methods

2.1 Chemicals

The ILs synthesized in the present work were prepared using the following reactants: oxalic acid (anhydrous, Fisher Scientific), salicylic acid (99%, Fisher Scientific), boric acid (99.99%, Fisher Scientific), lithium carbonate (99.99%, Sigma Aldrich), trimethyloctylammonium bromide ($[N_{1,1,1,8}]$Br, 97%, Tokyo Chemical Inc.), and triethylhexylammonium bromide ($[N_{2,2,2,6}]$Br, 98%, Tokyo Chemical Inc.). Dichloromethane (99.99%, dry, Arcos Organics) was used as solvent during the synthesis together with ultra-pure water (Milli-Q, electrical conductivity: 18.2 MΩ cm). As a reference IL, 1-hexyl-3-methylimidazolium bis(trifluoromethanesulfonyl)imide ([HMIM][TFSI], 99.99%, Tokyo Chemical Inc.) was employed.

2.2 Synthesis of Tetraalkylammonium Orthoborate Ionic Liquids

The synthesis of tetraalkylammonium orthoborate ILs was performed by modifying the approach developed by Shah et al. to obtain alkylphosphonium orthoborate ILs [58]. The synthesized cations and anions are displayed in Fig. 1, while the scheme of the synthesis is reported in Figure S.1 (Supporting Information).

A lithium orthoborate intermediate was synthesized in the first step (Step I in Figure S.1) by adding 40 mmol of oxalic or salicylic acid to an aqueous solution prepared by introducing 20 mmol of boric acid and 10 mmol lithium carbonate in 100 ml of ultra-pure water. After stirring the solution for 2 h at 333 K, water was removed under reduced pressure until precipitates began to form. The concentrate was then dried overnight at 368 K to completely remove any residual water. To carry out the metathesis reaction (Step II in Figure S.1) and obtain the final ILs, the synthesized lithium carbonate salts were then re-dissolved in 100 ml of ultra-pure water to which 20 mmol of $[N_{1,1,1,8}]$Br or $[N_{2,2,2,6}]$Br was added. The mixture was then stirred at room temperature for 2 h. The organic layer formed during the reaction was extracted with 60 ml of dichloromethane (DCM), and the washed 3 times with 100 ml of ultra-pure water. The DCM was then removed under reduced pressure, and the ILs was stored under reduced humidity (< 10%). Before further use, the ILs were dried at 413 K for 1 h to remove any residual solvents, and decompose any transition anionic complexes formed with exposure to water [89].

2.3 Characterization of Tetraalkylammonium Orthoborate ILs

The synthesized ILs were characterized by nuclear magnetic resonance (NMR) spectroscopy (Bruker Avance 400 spectrometer). The analyses (^{1}H, ^{13}C, ^{11}B) were carried out on as-synthesized ILs using acetone-d_6 as solvent. The density of the ILs was determined with an Anton Paar DMA500 densimeter under ambient conditions. The water content in the ILs was routinely quantified either by Karl Fischer (KF) titration using a Metrohm 317 coulometer or by NMR spectroscopy. Finally, the viscosity of the ILs was measured as a function of temperature (between room temperature and 353 K) using a cone-on-plate rheometer (ATS Nona Advanced Research, USA) at a shear rate between 1.2×10^{2} s^{-1} and 1.3×10^{3} s^{-1}. The results are displayed in the Figure S.2 (Supporting Information).

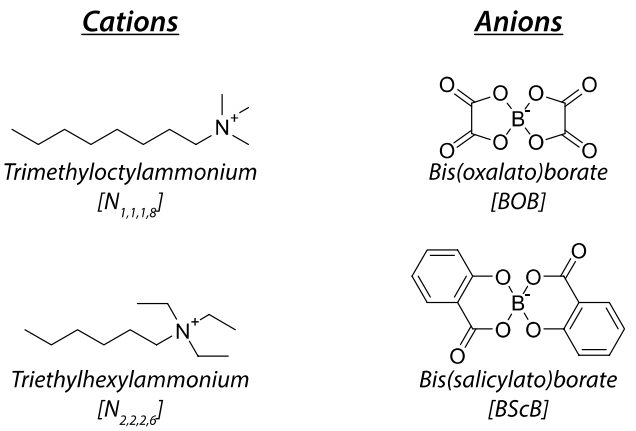

Fig. 1 Tetraalkylammonium cations and orthoborate anions synthesized in the present work

2.4 Tribological Testing

Reciprocating ball-on-flat tribological experiments were carried out with a Bruker UMT-2 tribometer in open air (relative humidity between 30 and 50%) and at elevated temperature (353 ± 3 K. This temperature was selected to perform tribological experiments in the mixed-lubrication regime, as discussed below, as well as compare the results with published works on other orthoborate-based ILs [88]). The contacting surfaces, namely 4 mm diameter balls and flat substrates, were both made of AISI 52100 steel (McMaster-Carr, USA). The steel substrates were first polished to achieve a final root-mean-square roughness of 2.1 ± 0.4 nm, as measured by atomic force microscopy over a 5×5 μm^2 area [85]. At the end of the polishing procedure, the specimens were sonicated for 10 min in light solvents (isopropanol, methanol, and acetone). All tribological experiments were performed under mixed-lubrication conditions ($0.06 < \lambda < 0.6$) [90], where the λ ratio was computed using the Hamrock and Dowson formula [91] and an upper bound for the pressure-viscosity coefficient of 12 GPa^{-1} [92]). The applied load was 5 N, which corresponds to a mean Hertzian contact pressure of 985 MPa, while the sliding speed was 1 mm/s and the stroke length was 4 mm. During the tests, the contact was fully immersed in the ILs. At the end of tribological experiments, the samples were thoroughly cleaned using acetone and sonicated in acetone for 10 min to remove the supernatant IL, and dried using a nitrogen (N5) stream. Prior to the tests, the ILs were left for at least 18 h at 373 K to remove absorbed water. During each 1-h tribological experiment an equal amount of the tested IL was left static in a vial in the same testing environment to quantify the water uptake in the ILs.

To determine the wear rate of 52100 steel discs after tribological tests, a Keyence VK X1100 optical profilometer was employed. The average specific wear rate (together with the corresponding standard deviation) was computed from the cross-sectional area of the wear track obtained from at least 50 line-scans across the worn region after subtraction of a linear background.

2.5 X-ray Photoelectron Spectroscopy Measurements

X-ray photoelectron spectroscopy (XPS) analyses were conducted on the steel discs after tribological testing. XPS measurements were carried out using a VersaProbe-IV XPS (ULVAC-PHI, Chanhassen USA) with a monochromatic Al Kα X-ray source. The base pressure in the XPS chamber was $< 1 \times 10^{-7}$ Pa. The spectrometer was calibrated according to ISO 15472:2001 with an accuracy of ± 0.1 eV. The spectra were acquired at an emission angle (EA) of 0° and using an incident X-ray beam of 20 µm in diameter. High-resolution spectra were collected in constant-analyzer-energy mode with a pass energy of 27 eV and a step size of 0.1 eV (full-width-at-half-maximum of the Ag $3d_{5/2}$ peak: 0.55 eV), while survey spectra were acquired using a pass energy of 140 eV and a step size of 1 eV. Secondary X-ray excited images (SXI) were used to locate regions of interest (*i.e.*, the wear tracks). The X-ray beam size was selected to collect data only within the wear track. When analyzing pure ILs, the electron neutralizer was used to compensate for sample charging. The spectra were processed using CasaXPS (v2.3.25, Casa Software Ltd, UK). The peak binding energies were referred to the aliphatic carbon signal at 285.0 eV. Before peak fitting, an iterated Shirley-Sherwood background subtraction was applied using a linear-squares algorithm. Quantitative analysis of XPS data was performed using the method described in Ref. [5], which relies on the first-principles method with Powell's equations [93]. The inelastic mean free path was computed using the Gries G1 formula [94].

3 Results and Discussion

Reciprocating ball-on-disc (52100-*vs.*-52100 steel) tribological tests were performed at 353 ± 3 K in the mixed-lubrication regime with neat $[N_{1,1,1,8}][BOB]$, $[N_{1,1,1,8}][BScB]$, and $[N_{2,2,2,6}][BOB]$. [HMIM][TFSI] was used as the reference IL, due to its extensive use in tribological studies [27]. Figure 2a displays the evolution of coefficient of friction over time represented as number of cycles, while the corresponding steady-state coefficient of friction values are presented in Fig. 2b. In the case of $[N_{1,1,1,8}][BOB]$ and $[N_{1,1,1,8}][BScB]$, a steady-state coefficient of friction of 0.114 ± 0.005 and 0.120 ± 0.003 was achieved after a running in period of 50 cycles and 190 cycles, respectively. While these values are significantly lower than the friction response achieved with neat [HMIM][TFSI], tribological experiments performed with $[N_{2,2,2,6}][BOB]$ resulted in a steady-state coefficient of friction slightly higher than the one of neat [HMIM][TFSI] after a running-in period of ~ 160 cycles. These results indicate that the substitution of the $[N_{1,1,1,8}]$ cation with the more symmetrical $[N_{2,2,2,6}]$ has a significant impact on the friction-reducing ability of tetraalkylammonium orthoborate ILs. This finding agrees well with previous reports indicating that increasing the length of the alkyl chains in the cations improves the lubricating properties of ILs at the macroscale [88, 95, 96]. However, the computation of the specific wear rate of steel discs after tribological experiments (Fig. 2c) shows that the anti-wear performance does not correlate with the chemical architecture of the cation, but it is influenced by the structure of the anion as the wear rate was higher in the case of the tests carried out in the presence of $[N_{1,1,1,8}][BScB]$ than in the experiments performed with [BOB]-containing ILs. Notably, the specific wear rate of 52100 steel discs used in experiments performed with neat

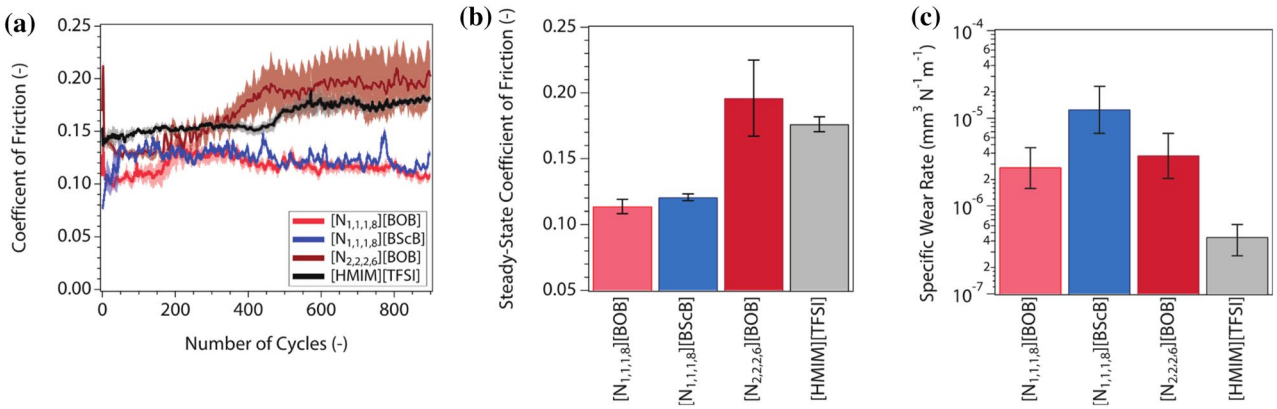

Fig. 2 **a** Coefficient of friction as a function of number of cycles obtained during reciprocating ball-on-disc (52100-vs.-52100 steel) tests carried out at 353 ± 3 K in neat $[N_{1,1,1,8}][BOB]$, $[N_{1,1,1,8}][BScB]$, $[N_{2,2,2,6}][BOB]$, and [HMIM][TFSI]. The steady-state coefficient of friction, computed by considering the last 200 cycles, and the specific wear rate are presented in (**b**) and (**c**), respectively

[HMIM][TFSI] is significantly lower than those observed with discs lubricated with any of the ammonium orthoborate ILs.

The analysis of the morphology of the wear tracks provided insights into the origin of this difference in specific wear rates (Fig. 3). While a primarily abrasive wear mechanism was observed in the case of the experiments performed with ammonium orthoborate ILs, an abrasive/corrosive wear mechanism is observed in neat [HMIM][TFSI], as indicated by the presence of pits and discoloration within the wear track. This is likely due to the formation of corrosive halogen halides as a result of the reaction between the halogenated [HMIM][TFSI] and atmospheric moisture [49, 50].

To gain insights into the chemical processes occurring at sliding interfaces and dictating the difference in friction response among the tetraalkylammonium orthoborate ILs synthesized in the present work, X-ray photoelectron spectroscopy (XPS) analyses were performed.

Before analyzing the steel discs used in tribological experiments, XPS measurements were performed on as-synthesized ILs as well as 52100 steel discs after polishing and aging (*i.e.*, after storing the discs in a desiccator for at least 3 days under reduced humidity to allow for the growth of native oxides). The high-resolution carbon 1 s spectrum (Fig. 4a) acquired on 52100 steel discs showed the presence of multiple components at 283.3 ± 0.1 eV (assigned to carbides [97, 98]), 285.0 ± 0.1 eV (assigned to aliphatic carbon [5, 97, 98]), and 286.5 ± 0.1 eV, 287.7 ± 0.1 eV, and 288.7 ± 0.2 eV (assigned to carbon bound to oxygen [5, 97, 98]). The asymmetric oxygen 1 s signal (Fig. 4b) includes components at 529.9 ± 0.1 eV, 531.1 ± 0.1 eV, 531.9 ± 0.1 eV, and 533.0 ± 0.1 eV, which were respectively assigned to iron oxide [5, 99–102], iron hydroxide [5, 99–101], iron carbonate [5, 99–104], and adsorbed water [5, 100–102]. The high-resolution spectrum of iron 2p (Fig. 4e) exhibited two peaks ($2p_{3/2}$ and $2p_{1/2}$) due to spin–orbit coupling. Curve synthesis, which was carried out only on the $2p_{3/2}$ peak, revealed the presence of the characteristic contributions of metallic iron at 706.5 ± 0.1 eV, iron (II) oxide at 709.2 ± 0.1 eV (together with its shake-up satellite at 714.7 eV), iron (III) oxide at 710.5 ± 0.1 eV, and iron oxide-hydroxide at 712.2 ± 0.2 eV [5, 100–102, 105–107].

XPS analyses were also performed on the as-synthesized ILs to obtain reference binding energies for the characteristic signals of the ions. Figure 4 displays the spectra acquired on $[N_{2,2,2,6}][BOB]$ as example (the XPS spectra of $[N_{1,1,1,8}][BOB]$ and $[N_{1,1,1,8}][BScB]$ are shown in Figure S.3 in the Supporting Information). The carbon 1 s spectrum shows three components at 285.0 ± 0.1 eV (assigned to aliphatic carbon [5, 97, 98]), 286.6 ± 0.1 eV (assigned to carbon bound to nitrogen [98]), and 289.6 ± 0.2 eV (assigned to carbon bound to oxygen [5, 97, 98]), while the oxygen 1 s exhibited two main peaks at 532.5 ± 0.1 eV and 533.5 ± 0.1 eV (assigned to oxygen bound to carbon in [BOB]) together with a component at 534.1 ± 0.1 eV due to water absorbed in the ILs. The characteristic signals of the cation and anion, namely the nitrogen 1 s and boron 1 s, were respectively detected at 402.3 ± 0.1 eV (in agreement with the nitrogen 1 s binding energy of other quaternary ammonium-containing ILs [108–110]) and 193.4 ± 0.1 eV

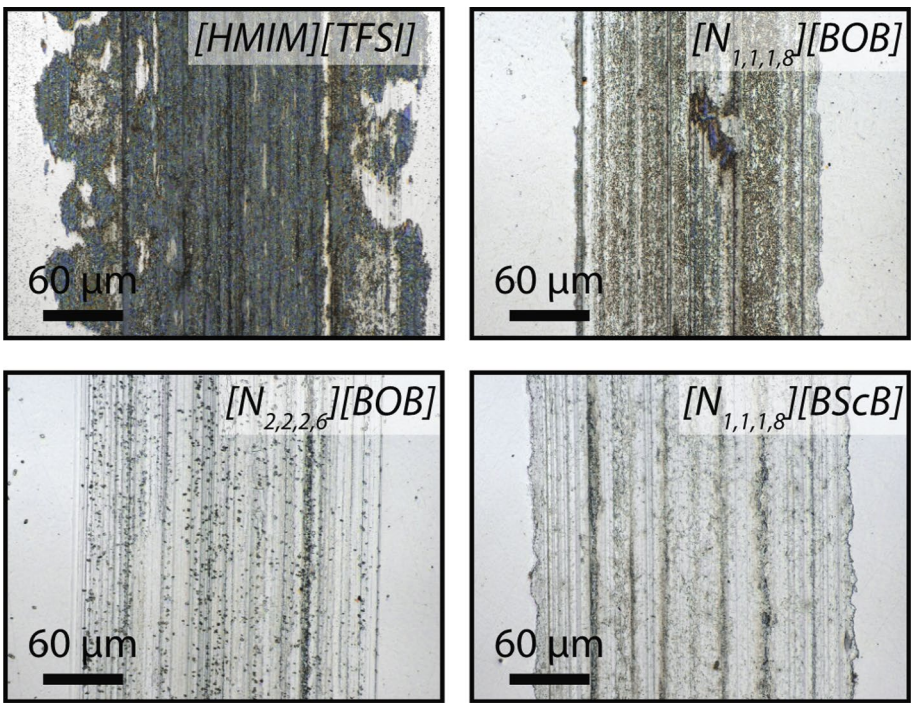

Fig. 3 Optical micrograph of 52100 steel discs after reciprocating ball-on-disc (52100-vs.-52100 steel) tests carried out at 353 ± 3 K in neat $[N_{1,1,1,8}][BOB]$, $[N_{1,1,1,8}][BScB]$, $[N_{2,2,2,6}][BOB]$, and [HMIM][TFSI]

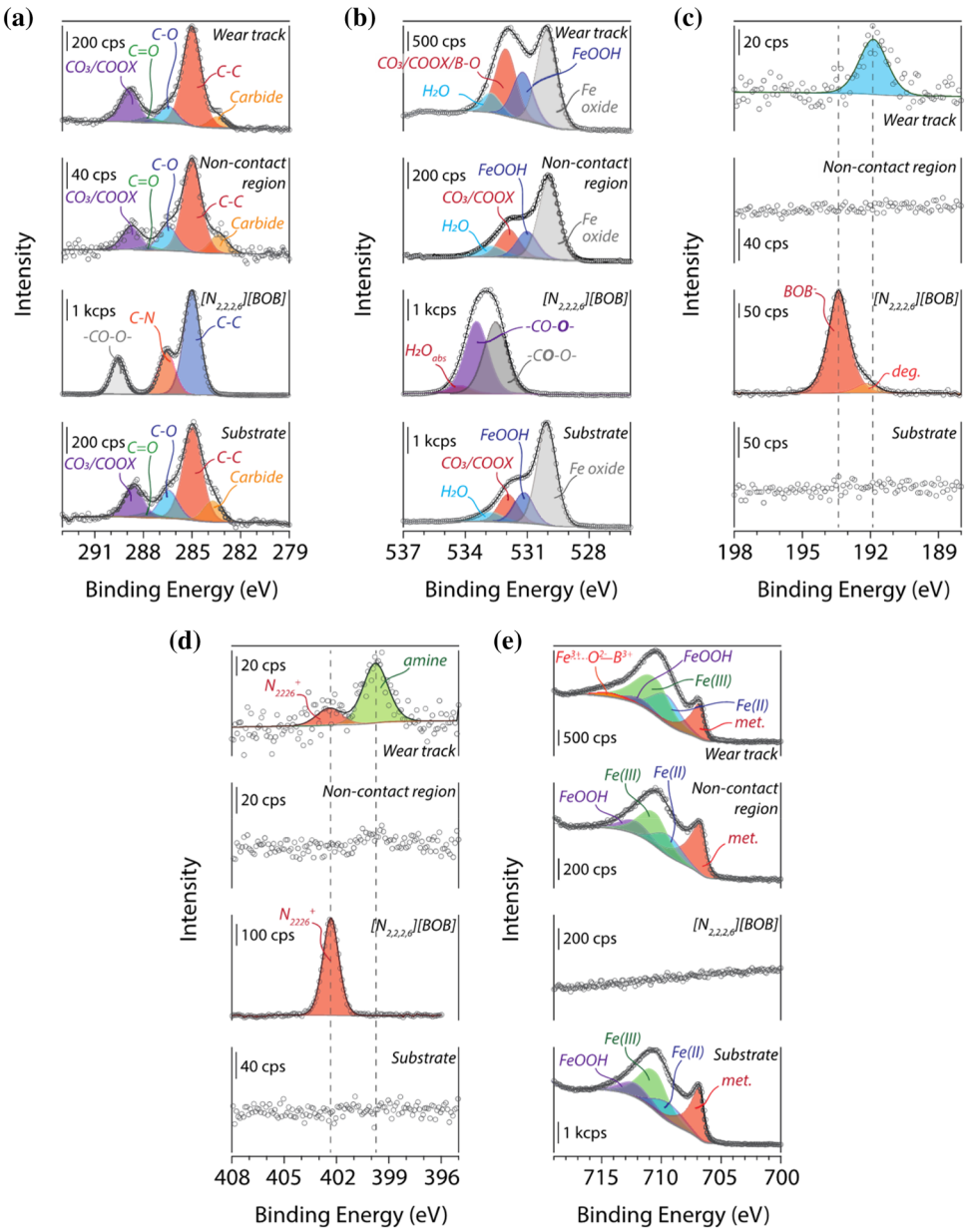

Fig. 4 High-resolution XPS spectra (carbon 1 s **a**; oxygen 1 s **b**; boron 1 s **c**; nitrogen 1 s **d**; and iron $2p_{3/2}$ **e**) acquired on as-prepared 52100 steel discs, as-synthesized $[N_{2,2,2,6}][BOB]$, and non-contact/contact regions of 52100 discs used for tribological testing in the presence of $[N_{2,2,2,6}][BOB]$

(close to the boron 1 s binding energy of tetrafluoroborate-containing ILs [108]). A small contribution to the boron 1 s signal was detected at 192.2 ± 0.2 eV, which can be assigned to species generated by the X-ray beam damage of the IL. The composition of $[N_{2,2,2,6}][BOB]$ computed on the basis of XPS results agrees well (within the experimental uncertainty) to the expected, nominal composition. While similar results were obtained with for $[N_{1,1,1,8}][BOB]$, it has to be highlighted that changing the chemical architecture of the anion (from [BOB] to [BScB]) resulted in a shift towards lower binding energy of the characteristic boron 1 s signal of the anion (from 193.4 ± 0.1 eV to 192.9 ± 0.1 eV) without any significant change of the position of the nitrogen 1 s signal of the cation (Figure S.3 in the Supporting Information). This result indicates that the introduction of aromatic rings in the anion increases the negative charge density on the boron atom without any significant charge-transfer from anion to cation, which is most likely due to the presence of alkyl chains around the cationic center that effectively shields it from the anion, in agreement with the previous work by of Blundell and Licence [108].

The XPS spectra acquired in the non-contact region of the steel discs used for tribological experiments in the presence of tetraalkylammonium orthoborate ILs exhibited carbon 1 s, oxygen 1 s, and iron 2p signals that were comparable to those collected on as-prepared steel substrates. In other words, no surface adsorption of ammonium or orthoborate ions was detected on steel. In contrast, the

acquisition of XPS spectra inside the wear tracks showed evidence of shear-induced mechanochemical reactions. First of all, the characteristic boron 1 s signal was detected at 191.9 ± 0.1 eV, which most closely corresponds to surface-adsorbed trivalent borate esters [12, 13, 111]. The presence of a boron-containing reaction product was corroborated by a new contribution in the iron 2p signal at 714.1 ± 0.2 eV, which is assigned to Fe^{3+}–O^{2-}–B^{3+} bonds [112–114]. Secondly, the most intense peak in the nitrogen 1 s was detected at 399.8 ± 0.1 eV, which corresponds to surface-bound amines [98, 115]. A minor component at 402.3 ± 0.1 eV is also present and was assigned to adsorbed alkylammonium cations. It must be highlighted that, while the sample cleaning procedure used in the present work completely removes the supernatant IL in the non-contact region, it might not be effective in washing off the IL present on any adsorbed reaction film in the wear track. In other words, the alkylammonium cations detected by XPS inside the worn region might be adsorbed on surface locations where trivalent borate esters and amines are present. Further investigations based on the use of spatially-resolved, surface-analytical measurements are required to shed light on the lateral arrangement of adsorbed IL ions within the wear track.

In addition to these spectral changes relative to the non-contact region, a much more intense peak assigned to carbon bonded to oxygen (*i.e.*, the CO_3/COOX synthetic peak) was also present in both carbon 1 s and oxygen 1 s spectra collected within the worn regions.

The surface coverage of boron- and nitrogen-containing compounds as well as species containing CO_3/COOX groups inside the wear track was found to strongly depend on the chemical structure of the ILs used in the tribological experiments and be correlated with the lubricating properties of the ILs. Figure 5a, b displays the ratio between the intensity of the boron signal assigned to adsorbed trivalent borate esters (nitrogen signal assigned to adsorbed amines) and the total intensity of the iron signal as a function of the steady-state coefficient of friction, while Fig. 5c presents the intensity of the CO_3/COOX synthetic peak in the carbon 1 s signal relative to the intensity of the iron signal as a function of the steady-state coefficient of friction. In the case of the experiments performed with ILs containing [$N_{1,1,1,8}$] cations, in which a very low steady-state coefficient of friction was achieved, a low surface coverage of boron, nitrogen, and CO_3/COOX functional groups was observed. In contrast, in the case of the IL that resulted in a higher steady-state friction coefficient, *i.e.*, [$N_{2,2,2,6}$][BOB], a much higher surface coverage of boron, nitrogen, and CO_3/COOX functional groups was detected, indicating that a significantly higher fraction of cations and anions tribochemically reacted on steel surfaces.

Based on the results of tribological experiments and XPS measurements, the following model is proposed to explain

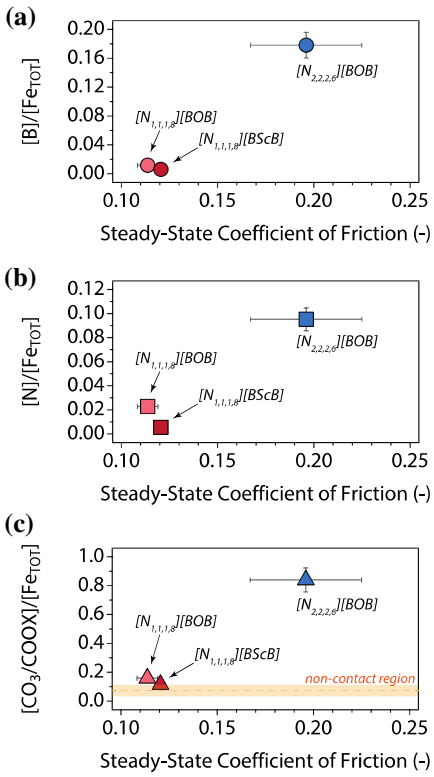

Fig. 5 **a** Ratio between the intensity of the boron 1 s signal assigned to adsorbed trivalent borate esters and the total intensity of the iron 2p signal as a function of the steady-state coefficient of friction; **b** ratio between the intensity of the nitrogen 1 s signal assigned to adsorbed amines and the total intensity of the iron 2p signal as a function of the steady-state coefficient of friction; **c** ratio between the intensity of the CO_3/COOX peak in the carbon 1 s signal and the total intensity of the iron 2p signal as a function of the steady-state coefficient of friction. The dash orange line and shaded area in (**c**) respectively correspond to the average and standard deviation intensity of the CO_3/COOX peak in the carbon 1 s signal relative to the total intensity of the iron 2p signal measured in the non-contact region of the samples

the tribological response of steel/steel contacts in the presence of tetraalkylammonium orthoborate ILs (Fig. 6). Under the contact conditions used in the present study, tetraalkylammonium orthoborate ILs with asymmetric cations (*i.e.*, [$N_{1,1,1,8}$]) do not form sacrificial tribofilms via shear-induced mechanochemical reactions (note: in the present work, the term "sacrificial" is used to describe surface layers formed on sliding surfaces as a result of tribochemical reactions, in a similar way to tribofilms formed by well-studied lubricant additives, such as zinc dialkyldithiophosphate [116]. This terminology thus highlights the difference between the layers formed by the shear-assisted interfacial reaction of lubricant additives and the boundary layers that can be formed by ILs, as discussed in the following). This supports the conclusions of previous studies that suggested the lubrication mechanisms of ILs to arise from their pressure-induced

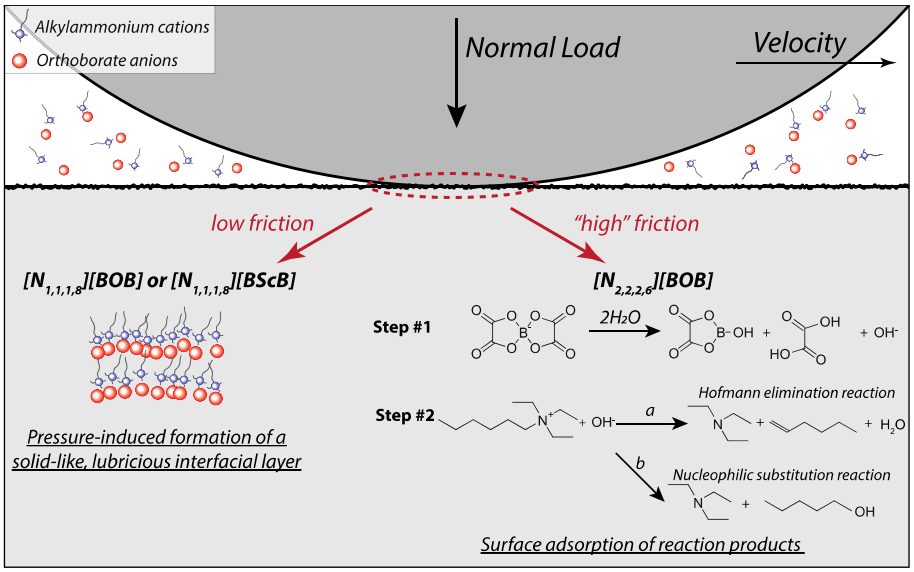

Fig. 6 Model proposed to describe the friction response of steel/steel contacts in the presence of tetraalkylammonium orthoborate ILs

morphological change, which results in the formation of a solid-like layered structure at the contact interface with low shear strength and difficult to displace [27, 28, 73–77]. However, in the case of IL with a more symmetric cation (*i.e.*, $[N_{2,2,2,6}]$[BOB]), the higher friction response is proposed to originate from the inability of this IL to create a lubricious, solid-like layer due to the reduced van der Waals interactions between the alkyl chains. The resulting hard/hard contact induces, in the presence of absorbed water, the cleavage of B–O bonds to generate trivalent borate esters along with oxalic acid and hydroxide ions (Step I in Fig. 6). The tribochemically formed oxalic acid then adsorbs onto the steel surface, contributing to the detected increase in the intensity of the peak assigned to carbon–oxygen bonds in the carbon 1 s and oxygen 1 s XPS signals collected within the wear tracks. Furthermore, as reported by Kleijwegt et al., the generation of hydroxides can lead to the degradation of alkylammonium cations through either Hoffmann elimination or nucleophilic substitution reactions (Step II in Fig. 6) [117]. In the case of the Hofmann elimination reaction (mechanism "*a*"), the hydroxides perform a nucleophilic attack on the β-hydrogen, leading to the release of a long alkene, a tertiary amine (which can adsorb on the steel surface, as indicated by XPS analyses) and water. In the less prevalent nucleophilic substitution reaction (mechanism "*b*"), the hydroxide reacts with the α-carbon of the long alkyl chain, generating an alcohol and a tertiary amine, which both adsorb on steel, as indicated by XPS measurements. While a similar set of degradation mechanisms was proposed in the case of phosphonium orthoborate ILs [88], the XPS analyses performed in the present study demonstrate, for the first time, that orthoborate ILs do not form inorganic iron borate glasses.

It has to be pointed out that, while the friction response of tetraalkylammonium orthoborate ILs was found to strongly depend on the cation structure (Fig. 2b), the anti-wear properties depend on the anion architecture (Fig. 2c). Even though $[N_{1,1,1,8}]$[BScB] has the highest viscosity among the ILs used in the present study (Figure S.2), which would result in the largest λ ratio, the profilometry results indicated that the highest specific wear rate was measured in tribological experiments performed in the presence of $[N_{1,1,1,8}]$[BScB] (Fig. 2c). This finding agrees well with the results reported by Shah et al. [58], who reported that, in the case of phosphonium orthoborate ILs comprising trihexyltetradecylphosphonium $[P_{6,6,6,14}]$ anion and [BOB] or [BScB] cations, the specific wear rate measured in pin-on-disk (steel-on-aluminum) experiments was higher in tests carried out with $[P_{6,6,6,14}]$[BScB] than in tests performed with $[P_{6,6,6,14}]$[BOB]. The variation of the anti-wear properties of tetraalkylammonium orthoborate ILs on the anion structure observed in the present work is proposed to originate from the effect of the anion architecture on the rate of formation of the protective boundary layer. Relative to ILs with [BOB] anions, the presence of aromatic rings in the chelated structure of [BScB] anions results in stronger intermolecular interactions between anions and a higher "rigidity" of the anionic moieties [57], which leads to a higher viscosity. As the self-diffusivity D_i of a species i with radius r_i is inversely proportional to the viscosity η according to Stokes–Einstein relation (*i.e.*, $D_i = M_i k_B T = \frac{k_B T}{6\pi\eta r_i}$,where M_i is the mobility of species i, k_B is the Boltzmann constant and T is the temperature), the ions in $[N_{1,1,1,8}]$[BScB] are less mobile compared to the ions in $[N_{1,1,1,8}]$[BOB], which agrees well with the lower self-diffusion coefficient of anions in $[P_{6,6,6,14}]$[BScB] than the one in $[P_{6,6,6,14}]$[BOB] measured by Filippov et al. using nuclear magnetic resonance (NMR) spectroscopy [118]. The resulting lower growth rate of

protective boundary layers in the experiments performed with $[N_{1,1,1,8}]$[BScB] relative to the tests carried out with $[N_{1,1,1,8}]$[BOB] causes stochastic friction spikes (Fig. 2a) and a higher specific wear rate. This finding is in agreement with a previous study performed by Li et al. [77], who performed in situ atomic force microscopy (AFM) experiments to evaluate the formation of a boundary layer by trihexyltetradecylphosphonium bis(2-ethylhexyl) phosphate ($[P_{6,6,6,14}]$[DEHP]) as a result of pressure-induced structural transition of confined IL molecules: the AFM results highlighted that decreasing the viscosity of the IL by performing the AFM experiments at higher temperatures leads to an increase in the growth rate of the protective, solid-like interfacial layer.

4 Conclusion

While ILs have been extensively evaluated for tribological applications, our understanding of their lubrication mechanism is still elusive. Here, we report a fundamental surface-analytical investigation of the mechanism by which a class of halogen-free ILs, namely tetraalkylammonium orthoborate ILs, reduces friction and wear at steel/steel sliding contacts. The tribological results indicate that increasing the length of the alkyl chains attached to ammonium cations improves the lubricating properties of the IL at the macroscale. XPS analyses shed light on the underpinning lubrication mechanisms and their strong dependency on the geometric asymmetry of the cation. The spectroscopic results revealed that the ILs with asymmetric ammonium cations containing a long alkyl chain (*i.e.*, $[N_{1,1,1,8}]$ cations) do not tribochemically react on steel surfaces to form sacrificial tribofilms, thus suggesting that the friction-reducing property of these ILs originates from their ability to undergo a pressure-induced morphological change leading to the generation of a lubricious, solid-like interfacial layered structure difficult to squeeze out from the contact region. Conversely, in the case of the IL having a more symmetric cation with a shorter alkyl chain (*i.e.*, $[N_{2,2,2,6}]$[BOB]), the higher friction response is proposed to originate from the IL inability to create a transient interfacial layer due to the reduced van der Waals interactions between the alkyl chains. The resulting hard/hard contact between the sliding surfaces leads to the mechanically-induced scission of boron-oxygen bonds in the presence of water, which not only results in the formation of trivalent borate esters and oxalic acid that adsorb on the steel surface, but also generates hydroxides that can trigger the degradation of alkylammonium cations and form tertiary amine able to absorb on steel. The results of this work establish links between the molecular structure of a class of halogen-free ILs, their lubricating performance, and lubrication mechanism, while also providing evidence for the existence of multiple mechanisms underpinning the promising lubricating properties of ILs in general.

Supplementary Information The online version contains supplementary material available at https://doi.org/10.1007/s11249-023-01714-7.

Acknowledgements The material is based upon work supported by the Welch Foundation (Grant No. F-2002-20190330) and the National Science Foundation Faculty Early Career Development Program (Grant No. 2042304). The acquisition of the VersaProbe-IV XPS was supported by the National Science Foundation Major Research Instrumentation program (Grant No. 2117623). F.M. acknowledges support from the 2018 Ralph E. Powe Junior Faculty Enhancement Award sponsored by the Oak Ridge Associated Universities (ORAU), and from the Walker Department of Mechanical Engineering and the Texas Materials Institute at the University of Texas at Austin. Last, but not least, this paper is dedicated to the memory of Prof. Anne Neville, whose contributions to tribology are long-standing and generous commitment to the development of the next-generation of scientists and engineers is endless.

Author Contributions JY: Conceptualization, Investigation, Data curation, Formal analysis, Writing—original draft, Writing—review & editing; H-ML: Investigation, Data curation, Writing—review & editing; FM: Conceptualization, Investigation, Formal analysis, Writing—original draft, Funding acquisition, Writing—review & editing.

Funding Welch Foundation, F-2002-20190330, National Science Foundation, 2042304 and 2117623, Oak Ridge Associated Universities, 2018 Ralph E. Powe Junior Faculty Enhancement Award.

Data Availability The datasets generated during and/or analysed during the current study are available from the corresponding author on reasonable request.

Declarations

Competing interest The authors declare no competing financial interests.

References

1. Pirro, D.M., Webster, M., Daschner, E.: Lubrication fundamentals : ExxonMobil Third edit. CRC Press, Taylor & Francis Group, CRC Press is an imprint of the Taylor & Francis Group, an informa business, Boca Raton (2016)
2. Spikes, H.: Low- and zero-sulphated ash, phosphorus and sulphur anti-wear additives for engine oils. Lubr. Sci. **20**, 103–136 (2008)
3. Tung, S.C.C., McMillan, M.L.L.: Automotive tribology overview of current advances and challenges for the future. Tribol. Int. **37**, 517–536 (2004). https://doi.org/10.1016/j.triboint.2004.01.013
4. Olree, R.M., McMillan, M.L.: How Much ZDP is Enough? SAE Tech. Pap, USA (2004)
5. Mangolini, F., Rossi, A., Spencer, N.: Chemical reactivity of triphenyl phosphorothionate (TPPT) with Iron: an ATR/FT-IR and XPS investigation. J. Phys. (2010). https://doi.org/10.1021/jp107617d
6. Mangolini, F., Rossi, A., Spencer, N.: Tribochemistry of triphenyl phosphorothionate (TPPT) by In situ attenuated total reflection (ATR/FT-IR) tribometry. J. Phys. (2012). https://doi.org/10.1021/jp209697a

7. Heuberger, R., Rossi, A., Spencer, N.D.: Reactivity of alkylated phosphorothionates with steel: a tribological and surface-analytical study. Lubr. Sci. **20**, 79–102 (2008). https://doi.org/10.1002/ls.56
8. Rossi, A., Piras, F.M., Kim, D., Gellman, A.J., Spencer, N.D.: Surface reactivity of tributyl thiophosphate: effects of temperature and mechanical stress. Tribol. Lett. **23**, 197–208 (2006). https://doi.org/10.1007/s11249-006-9051-6
9. Shah, F.U., Glavatskih, S., Antzutkin, O.N.: Boron in tribology: from borates to ionic liquids. Tribol. Lett. **51**, 281–301 (2013). https://doi.org/10.1007/s11249-013-0181-3
10. Kreuz, K.L., Fein, R.S., Dundy, M.: EP Films from borate lubricants. A S L E Trans. **10**, 67–76 (1967). https://doi.org/10.1080/05698196708972166
11. Liu, W., Jin, Z., Xue, Q.: The performance and antiwear mechanism of S-containing organic borate as an oil additive. Lubr. Sci. **7**, 49–60 (1994). https://doi.org/10.1002/ls.3010070105
12. Liu, W., Xue, Q., Zhang, X., Wang, H.: Effect of molecular structure of organic borates on their friction and wear properties. Lubr. Sci. **6**, 41–49 (1993). https://doi.org/10.1002/ls.3010060104
13. Philippon, D., De Barros-Bouchet, M.I., Lerasle, O., Le Mogne, T., Martin, J.M.: Experimental simulation of tribochemical reactions between borates esters and steel surface. Tribol. Lett. **41**, 73–82 (2011). https://doi.org/10.1007/s11249-010-9685-2
14. Pearson, R.G.: Hard and soft acids and bases, HSAB, part I, fundamental principles. J. Chem. Educ. **45**, 581–586 (1968)
15. Pearson, R.G.: Hard and soft acids and bases. J. Am. Chem. Soc. **85**, 3533–3539 (1963). https://doi.org/10.1021/ja00905a001
16. Pearson, R.G., Songstad, J.: Application of the principle of hard and soft acids and bases to organic chemistry. J. Am. Chem. Soc. **89**, 1827–1836 (1967). https://doi.org/10.1021/ja00984a014
17. Pearson, R.G.: Chemical Hardness. John Wiley & Sons, New York (1997)
18. Yao, J.B., Dong, J.X.: Improvement of hydrolytic stability of borate esters used as lubricant additives. Lubr. Eng. **51**, 475–479 (1995)
19. Zheng, Z., Shen, G., Wan, Y., Cao, L., Xu, X., Yue, Q., Sun, T.: Synthesis, hydrolytic stability and tribological properties of novel borate esters containing nitrogen as lubricant additives. Wear. **222**, 135–144 (1998). https://doi.org/10.1016/S0043-1648(98)00323-8
20. Yao, J.: Evaluation of sodium acetylacetonate as a synergist for arylamine antioxidants in synthetic lubricants. Tribol. Int. **30**, 795–799 (1997). https://doi.org/10.1016/S0301-679X(97)00046-7
21. Junbin, Y.: Antiwear function and mechanism of borate containing nitrogen. Tribol. Int. **30**, 387–389 (1997). https://doi.org/10.1016/S0301-679X(96)00060-6
22. Sharma, B.K., Doll, K.M., Heise, G.L., Myslinska, M., Erhan, S.Z.: Antiwear additive derived from soybean oil and boron utilized in a gear oil formulation. Ind. Eng. Chem. Res. **51**, 11941–11945 (2012). https://doi.org/10.1021/ie301519r
23. Li, W., Wu, Y., Wang, X., Liu, W.: Tribological study of boron-containing soybean lecithin as environmentally friendly lubricant additive in synthetic base fluids. Tribol. Lett. **47**, 381–388 (2012). https://doi.org/10.1007/s11249-012-9994-8
24. Zhou, Y., Qu, J.: Ionic Liquids as lubricant additives: a review. ACS Appl Mater Interfaces. **9**, 3209–3222 (2017). https://doi.org/10.1021/acsami.6b12489
25. A. Somers, P. Howlett, D. MacFarlane, M. Forsyth, A Review of Ionic Liquid Lubricants, Lubricants. 1 (2013) 3–21. http://www.mdpi.com/2075-4442/1/1/3.
26. Li, Z., Mangolini, F.: Recent advances in nanotribology of ionic liquids. Exp. Mech. (2021). https://doi.org/10.1007/s11340-021-00732-7
27. Espinosa-Marzal, R.M., Han, M., Arcifa, A., Spencer, N.D., Rossi, A.: Ionic liquids at interfaces and their tribological behavior. Ref. Modul. Chem. Mol. Sci. Chem. Eng. (2017). https://doi.org/10.1016/B978-0-12-409547-2.13857-0
28. Lhermerout, R., Diederichs, C., Perkin, S.: Are Ionic Liquids Good Boundary Lubricants? A Molecular Perspective. Lubricants. **6**(1), 9 (2018). https://doi.org/10.3390/lubricants6010009
29. MacFarlane, D.R., Kar, M., Pringle, J.M.: An Introduction to Ionic Liquids. In: MacFarlane, D.R., Kar, M., Pringle, J.M. (eds.) Fundamentals of Ionic Liquids: From Chemistry to Applicatio, pp. 1–25. Wiley-VCH Verlag GmbH & Co. KGaA, Weinheim (2017)
30. Minami, I.: Ionic liquids in tribology. Molecules **14**, 2286–2305 (2009). https://doi.org/10.3390/molecules14062286
31. Yu, B., Bansal, D.G., Qu, J., Sun, X., Luo, H., Dai, S., Blau, P.J., Bunting, B.G., Mordukhovich, G., Smolenski, D.J.: Oil-miscible and non-corrosive phosphonium-based ionic liquids as candidate lubricant additives. Wear **289**, 58–64 (2012). https://doi.org/10.1016/J.WEAR.2012.04.015
32. Qu, J., Truhan, J.J., Dai, S., Luo, H., Blau, P.J.: Ionic liquids with ammonium cations as lubricants or additives. Tribol. Lett. **22**, 207–214 (2006). https://doi.org/10.1007/s11249-006-9081-0
33. Kamimura, H., Kubo, T., Minami, I., Mori, S.: Effect and mechanism of additives for ionic liquids as new lubricants. Tribol. Int. **40**, 620–625 (2007). https://doi.org/10.1016/j.triboint.2005.11.009
34. Hjalmarsson, N., Wallinder, D., Glavatskih, S., Atkin, R., Aastrup, T., Rutland, M.W.: Weighing the surface charge of an ionic liquid. Nanoscale **7**, 16039–16045 (2015). https://doi.org/10.1039/c5nr03965g
35. Pilkington, G.A., Harris, K., Bergendal, E., Reddy, A.B., Palsson, G.K., Vorobiev, A., Antzutkin, O.N., Glavatskih, S., Rutland, M.W.: Electro-responsivity of ionic liquid boundary layers in a polar solvent revealed by neutron reflectance. J. Chem. Phys. **148**, 193806 (2018). https://doi.org/10.1063/1.5001551
36. Hjalmarsson, N., Bergendal, E., Wang, Y.-L., Munavirov, B., Wallinder, D., Glavatskih, S., Aastrup, T., Atkin, R., Furó, I., Rutland, M.W.: Electro-responsive surface composition and kinetics of an ionic liquid in a polar oil. Langmuir **35**, 15692–15700 (2019). https://doi.org/10.1021/acs.langmuir.9b02119
37. Watanabe, S., Pilkington, G.A., Oleshkevych, A., Pedraz, P., Radiom, M., Welbourn, R., Glavatskih, S., Rutland, M.W.: Interfacial structuring of non-halogenated imidazolium ionic liquids at charged surfaces: effect of alkyl chain length. Phys. Chem. Chem. Phys. **22**, 8450–8460 (2020). https://doi.org/10.1039/D0CP00360C
38. Li, H., Wood, R.J., Rutland, M.W., Atkin, R.: An ionic liquid lubricant enables superlubricity to be "switched on" in situ using an electrical potential. Chem. Commun. **50**, 4368 (2014)
39. Cooper, P.K., Li, H., Rutland, M.W., Webber, G.B., Atkin, R.: Tribotronic control of friction in oil-based lubricants with ionic liquid additives. Phys. Chem. Chem. Phys. **18**, 23657–23662 (2016). https://doi.org/10.1039/C6CP04405K
40. Li, H., Rutland, M.W., Atkin, R.: Ionic liquid lubrication: influence of ion structure, surface potential and sliding velocity. Phys. Chem. Chem. Phys. **15**, 14616–14623 (2013). https://doi.org/10.1039/C3CP52638K
41. Ye, C., Liu, W., Chen, Y., Yu, L.: Room-temperature ionic liquids: a novel versatile lubricant. Chem. Commun. (2001). https://doi.org/10.1039/B106935G
42. Otero, I., López, E.R., Reichelt, M., Fernández, J.: Friction and anti-wear properties of two tris(pentafluoroethyl)

trifluorophosphate ionic liquids as neat lubricants. Tribol. Int. **70**, 104–111 (2014). https://doi.org/10.1016/j.triboint.2013.10.002
43. Wang, H., Lu, Q., Ye, C., Liu, W., Cui, Z.: Friction and wear behaviors of ionic liquid of alkylimidazolium hexafluorophosphates as lubricants for steel/steel contact. Wear. **256**, 44–48 (2004). https://doi.org/10.1016/S0043-1648(03)00255-2
44. Lu, Q., Wang, H., Ye, C., Liu, W., Xue, Q.: Room temperature ionic liquid 1-ethyl-3-hexylimidazolium-bis(trifluoromethylsulfonyl)-imide as lubricant for steel–steel contact. Tribol. Int. **37**, 547–552 (2004). https://doi.org/10.1016/j.triboint.2003.12.003
45. Hernández Battez, A., Bartolomé, M., Blanco, D., Viesca, J.L., Fernández-González, A., González, R.: Phosphonium cation-based ionic liquids as neat lubricants: physicochemical and tribological performance. Tribol. Int. **95**, 118–131 (2016). https://doi.org/10.1016/j.triboint.2015.11.015
46. García, A., González, R., Hernández Battez, A., Viesca, J.L., Monge, R., Fernández-González, A., Hadfield, M.: Ionic liquids as a neat lubricant applied to steel–steel contacts. Tribol. Int. **72**, 42–50 (2014). https://doi.org/10.1016/j.triboint.2013.12.007
47. Munavirov, B., Black, J.J., Shah, F.U., Leckner, J., Rutland, M.W., Harper, J.B., Glavatskih, S.: The effect of anion architecture on the lubrication chemistry of phosphonium orthoborate ionic liquids. Sci. Rep. **11**, 24021 (2021). https://doi.org/10.1038/s41598-021-02763-5
48. Qu, J., Blau, P.J., Dai, S., Luo, H., Meyer, H.M.: Ionic liquids as novel lubricants and additives for diesel engine applications. Tribol. Lett. **35**, 181–189 (2009). https://doi.org/10.1007/s11249-009-9447-1
49. Freire, M.G., Neves, C.M.S.S., Marrucho, I.M., Coutinho, J.A.P., Fernandes, A.M.: Hydrolysis of tetrafluoroborate and hexafluorophosphate counter ions in imidazolium-based ionic liquids. J. Phys. Chem. A. **114**, 3744–3749 (2010). https://doi.org/10.1021/jp903292n
50. Petkovic, M., Seddon, K.R., Rebelo, L.P., Silva Pereira, C.: Ionic liquids: a pathway to environmental acceptability. Chem. Soc. Rev. **40**, 1383–1403 (2011). https://doi.org/10.1039/c004968a
51. Cvjetko Bubalo, M., Radošević, K., Radojčić Redovniković, I., Halambek, J., Gaurina Srček, V.: A brief overview of the potential environmental hazards of ionic liquids. Ecotoxicol. Environ. Saf. **99**, 1–12 (2014). https://doi.org/10.1016/j.ecoenv.2013.10.019
52. Stolte, S., Steudte, S., Areitioaurtena, O., Pagano, F., Thöming, J., Stepnowski, P., Igartua, A.: Ionic liquids as lubricants or lubrication additives: an ecotoxicity and biodegradability assessment. Chemosphere **89**, 1135–1141 (2012). https://doi.org/10.1016/J.CHEMOSPHERE.2012.05.102
53. Yan, J., Mangolini, F.: Engineering encapsulated ionic liquids for next-generation applications. RSC Adv. **11**, 36273–36288 (2021). https://doi.org/10.1039/d1ra05034f
54. Guo, H., Iglesias, P.: Tribological behavior of ammonium-based protic ionic liquid as lubricant additive. Friction. **9**, 169–178 (2021). https://doi.org/10.1007/s40544-020-0378-z
55. Patel, A., Guo, H., Iglesias, P.: Study of the lubricating ability of protic ionic liquid on an aluminum–steel contact. Lubricants. **6**(3), 66 (2018). https://doi.org/10.3390/lubricants6030066
56. Khan, A., Yasa, S.R., Gusain, R., Khatri, O.P.: Oil-miscible, halogen-free, and surface-active lauryl sulphate-derived ionic liquids for enhancement of tribological properties. J. Mol. Liq. **318**, 114005 (2020). https://doi.org/10.1016/J.MOLLIQ.2020.114005
57. Gusain, R., Khatri, O.P.: Halogen-free ionic liquids: Effect of chelated orthoborate anion structure on their lubrication properties. RSC Adv. **5**, 25287–25294 (2015). https://doi.org/10.1039/c5ra03092g
58. Shah, F.U., Glavatskih, S., MacFarlane, D.R., Somers, A.E., Forsyth, M., Antzutkin, O.N.: Novel halogen-free chelated orthoborate-phosphonium ionic liquids: synthesis and tribophysical properties. Phys. Chem. Chem. Phys. **13**, 12865–12873 (2011). https://doi.org/10.1039/c1cp21139k
59. Wu, J., Lu, X., Feng, X., Shi, Y.: Halogen-free ionic liquids as excellent lubricants for PEEK-stainless steel contacts at elevated temperatures. Tribol. Int. **104**, 1–9 (2016). https://doi.org/10.1016/j.triboint.2016.08.009
60. Khatri, P.K., Joshi, C., Thakre, G.D., Jain, S.L.: Halogen-free ammonium-organoborate ionic liquids as lubricating additives: the effect of alkyl chain lengths on the tribological performance. New J. Chem. **40**, 5294–5299 (2016). https://doi.org/10.1039/c5nj02225h
61. Zhou, Y., Dyck, J., Graham, T.W., Luo, H., Leonard, D.N., Qu, J.: Ionic liquids composed of phosphonium cations and organophosphate, carboxylate, and sulfonate anions as lubricant antiwear additives. Langmuir **30**, 13301–13311 (2014). https://doi.org/10.1021/la5032366
62. Gusain, R., Dhingra, S., Khatri, O.P.: Fatty-acid-constituted halogen-free ionic liquids as renewable, environmentally friendly, and high-performance lubricant additives. Ind. Eng. Chem. Res. **55**, 856–865 (2016). https://doi.org/10.1021/acs.iecr.5b03347
63. Gusain, R., Singh, R., Sivakumar, K.L.N., Khatri, O.P.: Halogen-free imidazolium/ammonium-bis(salicylato)borate ionic liquids as high performance lubricant additives. RSC Adv. **4**, 1293–1301 (2014). https://doi.org/10.1039/C3RA43052A
64. Gusain, R., Bakshi, P.S., Panda, S., Sharma, O.P., Gardas, R., Khatri, O.P.: Physicochemical and tribophysical properties of trioctylalkylammonium bis(salicylato)borate (N888n-BScB) ionic liquids: effect of alkyl chain length. Phys. Chem. Chem. Phys. **19**, 6433–6442 (2017). https://doi.org/10.1039/C6CP05990B
65. Taher, M., Shah, F.U., Filippov, A., de Baets, P., Glavatskih, S., Antzutkin, O.N.: Halogen-free pyrrolidinium bis(mandelato) borate ionic liquids: some physicochemical properties and lubrication performance as additives to polyethylene glycol. RSC Adv. **4**, 30617–30623 (2014). https://doi.org/10.1039/C4RA02551B
66. Qu, J., Bansal, D.G., Yu, B., Howe, J.Y., Luo, H., Dai, S., Li, H., Blau, P.J., Bunting, B.G., Mordukhovich, G., Smolenski, D.J.: Antiwear performance and mechanism of an oil-miscible ionic liquid as a lubricant additive. ACS Appl. Mater. Interfaces. **4**, 997–1002 (2012). https://doi.org/10.1021/am201646k
67. Qu, J., Luo, H., Chi, M., Ma, C., Blau, P.J., Dai, S., Viola, M.B.: Comparison of an oil-miscible ionic liquid and ZDDP as a lubricant anti-wear additive. Tribol. Int. **71**, 88–97 (2014). https://doi.org/10.1016/j.triboint.2013.11.010
68. González, R., Viesca, J.L., Battez, A.H., Hadfield, M., Fernández-González, A., Bartolomé, M.: Two phosphonium cation-based ionic liquids as lubricant additive to a polyalphaolefin base oil. J. Mol. Liq. **293**, 111536 (2019). https://doi.org/10.1016/j.molliq.2019.111536
69. Fu, X., Sun, L., Zhou, X., Li, Z., Ren, T.: Tribological study of oil-miscible quaternary ammonium phosphites ionic liquids as lubricant additives in PAO. Tribol. Lett. **60**, 23 (2015). https://doi.org/10.1007/s11249-015-0596-0
70. Fan, M., Yang, D., Wang, X., Liu, W., Fu, H.: DOSS– based QAILs: as both neat lubricants and lubricant additives with excellent tribological properties and good detergency. Ind. Eng. Chem. Res. **53**, 17952–17960 (2014). https://doi.org/10.1021/ie502849w
71. Barnhill, W.C., Qu, J., Luo, H., Meyer, H.M., Ma, C., Chi, M., Papke, B.L.: Phosphonium-organophosphate ionic liquids as lubricant additives: effects of cation structure on physicochemical and tribological characteristics. ACS Appl. Mater. Interfaces. **6**, 22585–22593 (2014). https://doi.org/10.1021/am506702u

72. Barnhill, W.C., Luo, H., Meyer, H.M., Ma, C., Chi, M., Papke, B.L., Qu, J.: Tertiary and quaternary ammonium-phosphate ionic liquids as lubricant additives. Tribol. Lett. (2016). https://doi.org/10.1007/s11249-016-0707-6
73. Perkin, S., Crowhurst, L., Niedermeyer, H., Welton, T., Smith, A.M., Gosvami, N.N.: Self-assembly in the electrical double layer of ionic liquids. Chem Commun. **47**, 6572–6574 (2011). https://doi.org/10.1039/C1CC11322D
74. Werzer, O., Atkin, R.: Interactions of adsorbed poly(ethylene oxide) mushrooms with a bare silica-ionic liquid interface. Phys. Chem. Chem. Phys. **13**, 13479–13485 (2011). https://doi.org/10.1039/C1CP20174C
75. Espinosa-Marzal, R.M., Arcifa, A., Rossi, A., Spencer, N.D.D.: Microslips to "avalanches" in confined, molecular layers of ionic liquids. J. Phys. Chem. Lett. **5**, 179–184 (2013). https://doi.org/10.1021/jz402451v
76. Smith, A.M., Lovelock, K.R.J., Gosvami, N.N., Welton, T., Perkin, S.: Quantized friction across ionic liquid thin films. Phys. Chem. Chem. Phys. **15**, 15317–15320 (2013). https://doi.org/10.1039/c3cp52779d
77. Li, Z., Morales-Collazo, O., Chrostowski, R., Brennecke, J.F., Mangolini, F.: In situ nanoscale evaluation of pressure-induced changes in structural morphology of phosphonium phosphate ionic liquid at single-asperity contacts. RSC Adv. **12**, 413–419 (2021). https://doi.org/10.1039/d1ra08026a
78. Li, Z., Dolocan, A., Morales-Collazo, O., Sadowski, J.T., Celio, H., Chrostowski, R., Brennecke, J.F., Mangolini, F.: Lubrication mechanism of phosphonium phosphate ionic liquid in nanoscale single-asperity sliding contacts. Adv. Mater. Interfaces. **7**, 2000426 (2020). https://doi.org/10.1002/admi.202000426
79. Qu, J., Blau, P.J., Dai, S., Luo, H., Meyer, H.M., Truhan, J.J.: Tribological characteristics of aluminum alloys sliding against steel lubricated by ammonium and imidazolium ionic liquids. Wear. **267**, 1226–1231 (2009). https://doi.org/10.1016/j.wear.2008.12.038
80. Guo, W., Zhou, Y., Sang, X., Leonard, D.N., Qu, J., Poplawsky, J.D.: Atom probe tomography unveils formation mechanisms of wear-protective tribofilms by ZDDP, ionic liquid, and their combination. ACS Appl Mater Interfaces. **9**, 23152–23163 (2017). https://doi.org/10.1021/acsami.7b04719
81. Qu, J., Chi, M., Meyer, H.M., Blau, P.J., Dai, S., Luo, H.: Nanostructure and composition of Tribo-boundary films formed in ionic liquid lubrication. Tribol. Lett. **43**, 205–211 (2011). https://doi.org/10.1007/s11249-011-9800-z
82. Minami, I., Inada, T., Sasaki, R., Nanao, H.: Tribo-chemistry of phosphonium-derived ionic liquids. Tribol. Lett. **40**, 225–235 (2010). https://doi.org/10.1007/s11249-010-9626-0
83. Zhou, F., Liang, Y., Liu, W.: Ionic liquid lubricants: designed chemistry for engineering applications. Chem. Soc. Rev. **38**, 2590–2599 (2009). https://doi.org/10.1039/B817899M
84. Weng, L.J., Liu, X.Q., Liang, Y.M., Xue, Q.J.: Effect of tetraalkylphosphonium based ionic liquids as lubricants on the tribological performance of a steel-on-steel system. Tribol. Lett. **26**, 11–17 (2007). https://doi.org/10.1007/s11249-006-9175-8
85. Li, Z., Celio, H., Dolocan, A., Molina, N., Kershaw, J., Morales-Collazo, O., Brennecke, J.F., Mangolini, F.: Tuning the surface reactivity and tribological performance of phosphonium-based ionic liquid at steel/steel interfaces by bromide/phosphate anion mixtures. Appl. Surf. Sci. (2021). https://doi.org/10.1016/j.apsusc.2021.151245
86. Guan, B., Pochopien, B.A., Wright, D.S.: The chemistry, mechanism and function of tricresyl phosphate (TCP) as an anti-wear lubricant additive. Lubr. Sci. **28**, 257–265 (2015). https://doi.org/10.1002/ls.1327
87. Osei-Agyemang, E., Berkebile, S., Martini, A.: Decomposition mechanisms of anti-wear lubricant additive tricresyl phosphate on iron surfaces using dft and atomistic thermodynamic studies. Tribol. Lett. (2018). https://doi.org/10.1007/s11249-018-0998-x
88. Rohlmann, P., Watanabe, S., Shimpi, M.R., Leckner, J., Harper, J.B., Rutland, M.W., Glavatskih, S., Harper, J.B., Glavatskih, S.: Boundary lubricity of phosphonium bisoxalatoborate ionic liquids. Tribol. Int. **161**, 107075 (2021). https://doi.org/10.1016/j.triboint.2021.107075
89. Shimpi, M.R., Rohlmann, P., Shah, F.U., Glavatskih, S., Antzutkin, O.N.: Transition anionic complex in trihexyl(tetradecyl) phosphonium-bis(oxalato)borate ionic liquid - revisited. Phys. Chem. Chem. Phys. **23**, 6190–6203 (2021). https://doi.org/10.1039/d0cp05845a
90. Spikes, H.A.: Sixty years of EHL. Lubr. Sci. **18**, 265–291 (2006). https://doi.org/10.1002/ls.23
91. Hamrock, B.J., Dowson, D.: Isothermal elastohydrodynamic lubrication of point contacts: part 1—theoretical formulation. J. Lubr. Technol. **98**, 223–228 (1976). https://doi.org/10.1115/1.3452801
92. Pensado, A.S., Comuñas, M.J.P., Fernández, J.: The pressure-viscosity coefficient of several ionic liquids. Tribol. Lett. **31**, 107–118 (2008). https://doi.org/10.1007/s11249-008-9343-0
93. Powell, C.J.: The Physical Basis for Quantitative Surface Analysis by Auger Electron Spectroscopy and X-ray Photoelectron Spectroscopy. In: McIntyre, N.S. (ed.) Quant, pp. 5–30. American Society for Testing and Materials, Surf. Anal. Mater. (1978)
94. Tanuma, S.: Electron attenuation lengths. In: Briggs, D., Grant, J.T. (Eds.), Surf. Anal. by Auger X-Ray Photoelectron Spectroscopy, pp. 259–294. IM Publications, Chichester (UK) (2003)
95. Smith, A.M., Parkes, M.A., Perkin, S.: Molecular friction mechanisms across nanofilms of a bilayer-forming ionic liquid. J. Phys. Chem. Lett. **5**, 4032–4037 (2014). https://doi.org/10.1021/jz502188g
96. Xiao, H., Guo, D., Liu, S., Pan, G., Lu, X.: Film thickness of ionic liquids under high contact pressures as a function of alkyl chain length. Tribol. Lett. **41**, 471–477 (2011). https://doi.org/10.1007/s11249-010-9729-7
97. Moulder, J.F., Stickle, W.F., Sobol, P.E., Bomben, K.D.: Handbook of X-ray Photoelectron Spectroscopy. Perkin-Elmer Corporation, Physical Electronics Division, Eden Prairie (1992)
98. Beamson, G., Briggs, D.: High Resolution XPS of Organic Polymers: The Scienta ESCA300 Database. John Wiley & Sons, Chichester (UK) (1992)
99. G. Bhargava, I. Gouzman, C.M. Chun, T.A. Ramanarayanan, S.L. Bernasek, Characterization of the "native" surface thin film on pure polycrystalline iron: A high resolution XPS and TEM study, Appl. Surf. Sci. 253 (2007) 4322–4329. http://www.sciencedirect.com/science/article/B6THY-4M7CD68-1/2/a3740dd824beb0a6f4b8183ca8a9849d.
100. C.R. Brundle, T.J. Chuang, K. Wandelt, Core and valence level photoemission studies of iron oxide surfaces and the oxidation of iron, Surf. Sci. 68 (1977) 459–468. http://www.sciencedirect.com/science/article/B6TVX-46SX0F3-1GM/2/f3aaff2bd84e32f28113ece1c7039ede.
101. Olla, M., Navarra, G., Elsener, B., Rossi, A.: Nondestructive in-depth composition profile of oxy-hydroxide nanolayers on iron surfaces from ARXPS measurement. Surf. Interface Anal. **38**, 964–974 (2006). https://doi.org/10.1002/sia.2362
102. M. Eglin, A. Rossi, N.D. Spencer, X-ray Photoelectron Spectroscopy Analysis of Tribostressed Samples in the Presence of ZnDTP: A Combinatorial Approach, Tribol. Lett. 15 (2003) 199–209. http://www.springerlink.com/content/jg086j515145xq64.
103. S.L. Wu, Z.D. Cui, F. He, Z.Q. Bai, S.L. Zhu, X.J. Yang, Characterization of the surface film formed from carbon dioxide corrosion on N80 steel, Mater. Lett. 58 (2004) 1076–1081. http://www.sciencedirect.com/science/article/B6TX9-49MX0HP-2/2/4b6a391704183884186b4ee1963d55f2.

104. J.K. Heuer, J.F. Stubbins, An XPS characterization of FeCO3 films from CO2 corrosion, Corros. Sci. 41 (1999) 1231–1243. http://www.sciencedirect.com/science/article/B6TWS-3WM5H6X-1/2/d821079dcac0e54352ade1ced4db10e2.
105. P. de Donato, C. Mustin, R. Benoit, R. Erre, Spatial distribution of iron and sulphur species on the surface of pyrite, Appl. Surf. Sci. 68 (1993) 81–93. http://www.sciencedirect.com/science/article/B6THY-46CC3KT-6Y/2/de3bf1c40bcc0a20adad2febb93c0fbc.
106. M. Descostes, F. Mercier, N. Thromat, C. Beaucaire, M. Gautier-Soyer, Use of XPS in the determination of chemical environment and oxidation state of iron and sulfur samples: constitution of a data basis in binding energies for Fe and S reference compounds and applications to the evidence of surface species of an oxidized py, Appl. Surf. Sci. 165 (2000) 288–302. http://www.sciencedirect.com/science/article/B6THY-40WDTRR-6/2/6312a5964ec5f1d3581f72f32eec20a6.
107. R.P. Gupta, S.K. Sen, Calculation of multiplet structure of core p -vacancy levels. II, Phys. Rev. B. 12 (1975) 15. http://link.aps.org/abstract/PRB/v12/p15.
108. Blundell, R.K., Licence, P.: Quaternary ammonium and phosphonium based ionic liquids: a comparison of common anions. Phys. Chem. Chem. Phys. **16**, 15278–15288 (2014). https://doi.org/10.1039/c4cp01901f
109. Gabler, C., Tomastik, C., Brenner, J., Pisarova, L., Doerr, N., Allmaier, G.: Corrosion properties of ammonium based ionic liquids evaluated by SEM-EDX, XPS and ICP-OES. Green Chem. **13**, 2869–2877 (2011). https://doi.org/10.1039/c1gc15148g
110. Arellanes-Lozada, P., Olivares-Xometl, O., Likhanova, N.V., Lijanova, I.V., Vargas-García, J.R., Hernández-Ramírez, R.E.: Adsorption and performance of ammonium-based ionic liquids as corrosion inhibitors of steel. J. Mol. Liq. **265**, 151–163 (2018). https://doi.org/10.1016/J.MOLLIQ.2018.04.153
111. Baldwin, B.A.: Relative antiwear efficiency of boron and sulfur surface species. Wear **45**, 345–353 (1977). https://doi.org/10.1016/0043-1648(77)90025-4
112. Spadaro, F., Rossi, A., Lainé, E., Woodward, P., Spencer, N.D.: Tuning the surface chemistry of lubricant-derived phosphate thermal films: the effect of boron. Appl. Surf. Sci. **396**, 1251–1263 (2017). https://doi.org/10.1016/J.APSUSC.2016.11.124
113. Kumari, K., Ram, S., Kotnala, R.K.: Self-controlled growth of Fe3BO6 crystallites in shape of nanorods from iron-borate glass of small templates. Mater. Chem. Phys. **129**, 1020–1026 (2011). https://doi.org/10.1016/j.matchemphys.2011.05.051
114. Spadaro, F., Rossi, A., Ramakrishna, S.N., Lainé, E., Woodward, P., Spencer, N.D.: Understanding complex tribofilms by means of H3BO3-B2O3 model glasses. Langmuir **34**, 2219–2234 (2018). https://doi.org/10.1021/ACS.LANGMUIR.7B01795/ASSET/IMAGES/LARGE/LA-2017-017959_0009.JPEG
115. Artyushkova, K.: Misconceptions in interpretation of nitrogen chemistry from x-ray photoelectron spectra. J. Vac. Sci. Technol. A. **38**, 031002 (2020). https://doi.org/10.1116/1.5135923
116. Zhang, J., Spikes, H.: On the mechanism of ZDDP antiwear film formation. Tribol. Lett. **63**, 1–15 (2016). https://doi.org/10.1007/s11249-016-0706-7
117. Kleijwegt, R.J.T., Winkenwerder, W., Baan, W., van der Schaaf, J.: Degradation kinetics and solvent effects of various long-chain quaternary ammonium salts. Int. J. Chem. Kinet. **54**, 16–27 (2022). https://doi.org/10.1002/kin.21537
118. Filippov, A., Munavirov, B., Glavatskih, S., Shah, F.U., Antzutkin, O.N.: Diffusion of Ions in phosphonium orthoborate ionic liquids studied by 1H and 11B pulsed field gradient NMR. Front. Chem. **8**, 1–9 (2020). https://doi.org/10.3389/fchem.2020.00119

Authors and Affiliations

Jieming Yan[1,2] · Hsu-Ming Lien[1,2] · Filippo Mangolini[1,3]

✉ Filippo Mangolini
filippo.mangolini@austin.utexas.edu

[1] Texas Materials Institute, The University of Texas at Austin, Austin, TX 78712, USA

[2] Materials Science and Engineering Program, The University of Texas at Austin, Austin, TX 78712, USA

[3] Walker Department of Mechanical Engineering, The University of Texas at Austin, Austin, TX 78712, USA